

## SHEAR FAILURE ANALYSIS OF HIGH STRENGTH SELF COMPACTING CONCRETE BEAMS

**KANWAR JEET SINGH**  
Research Scholar, Department  
of Civil Engineering,  
Punjab Technical University,  
Jalandhar.  
Guru Nanak Dev Engineering  
College, Ludhiana.  
Kanwarjeet\_b@yahoo.com

**Dr. RAJESH KUMAR**  
Professor, Department of  
Civil Engineering,  
CCET Chandigarh.  
[rajshaastha@rediffmail.com](mailto:rajshaastha@rediffmail.com)

**Dr. S.P. SINGH**  
Professor, Department of  
Civil Engineering,  
NIT Jalandhar  
[spsingh@nitj.ac.in](mailto:spsingh@nitj.ac.in)

**Dr. HARVINDER SINGH**  
Associate Professor,  
Department of Civil  
Engineering,  
GNDEC, Ludhiana.  
[hs.gndec@gmail.com](mailto:hs.gndec@gmail.com)

### ABSTRACT:

*The paper presents the results of experimental investigation conducted to investigate the shear strength of high strength Self Compacting Concrete (SCC) beams. The aim was to investigate the effect of longitudinal reinforcement and shear span on the shear strength. Keeping the section constant at 150 x 300 mm, the shear span to depth ratio (a/d) was varied between 1.5 to 3.5. Concrete mix of M60 grade was selected with five longitudinal reinforcement percentages of 0.55%, 1.0%, 2.1%, 3.1% and 4.1%. The performance of High Strength SCC beams was evaluated based on the results of crack pattern, deflection, shear cracking load, ultimate shear resistance, and failure modes. The applicability of concrete design standards of different countries and expressions proposed by researchers to calculate the concrete contribution to shear resistance of Reinforced Concrete (RC) beams without stirrups was investigated. Shear strength results obtained from experimental investigations had been compared with their corresponding predicted values. Results of this study indicate that SCC possesses comparable or even better shear strength than normally vibrated RC beams.*

**Keywords:** Aggregate interlocking, Self-compacting concrete, Flexure shear crack, Compression zone, Shear span to depth ratio, Dowel action, Arch action mechanism

### INTRODUCTION

Self Compacting Concrete (SCC) is highly flow able and easily spreadable through congested reinforcement and conveniently serves the dual purpose of high strength and self compaction. It differs from vibrated concrete (VC) mixtures by the increased amount of fine aggregates and fillers and addition of a superplasticizer to increase workability. In high strength concrete the cracks tend to propagate through aggregates rather than around the

aggregates as in normal strength concrete, resulting in a much smoother shear failure surface. The shear carried by aggregate interlock tends to decrease with increase in concrete strength. This means that contribution to shear strength due to aggregate interlocking is much less or negligible in high strength SCC as compared to normal strength SCC. Due to difference in coarse aggregate content, the shear behavior of SCC and VC may differ in normal strength range, but is expected to be same in high strength range. Mphonde<sup>[1]</sup> conducted experimental investigations on concrete beams without shear reinforcement and with compressive strength varying between 21 to 83 MPa. It was concluded that the effect of concrete strength becomes more significant with smaller a/d ratios and failures became more sudden and explosive with higher concrete strength. Beams with small a/d values showed greater scatter in the results possibly due to variations in the failure modes. Experimental investigation conducted on both SCC and VC beams<sup>[2]</sup> with same compressive strength of 45 MPa indicated upto 17% reduced shear strength of SCC beams. On the other hand another comparative experimental study conducted by Lachemi<sup>[3]</sup> on SCC and VC beams reported a mere 5% difference in shear capacity. Beams were without shear reinforcement and compressive strength ranging between 50 – 58 MPa. Experimental and theoretical study conducted on precast, pre-stressed beams<sup>[4]</sup> reported 10% reduction in shear

capacity for beams made with SCC as compared to VC with the same compressive strength.

With a large scatter in test results, it is hardly convincing that SCC has a poor shear resistance as compared to VC, particularly in high compressive strength range. This paper presents the results of an investigation into the overall shear behavior of 15 full-scale longitudinally reinforced concrete beams made with high strength SCC. To study the shear failure mechanism in a better way, no shear reinforcement is provided in any of the beams<sup>[5]</sup>. The two test parameters are shear span to depth ratio and longitudinal reinforcement percentage. Experimentally investigated shear strength is compared with code based design equations of different standards and shear strength expressions presented by various researchers.

**1. EXPERIMENTAL PROGRAM**

**1.1 Description of Test Beams**

A total of 15 longitudinally reinforced SCC beams were cast with shear span to depth ratio ranging between 1.5 to 3.5.

Table 1. Detail of beam specimens

Beam specimen designation	Effective length(mm)	a/d	Longitudinal steel (bar detail)	Longitudinal steel percentage ( $\rho_w=100A_{st}/bd$ )
A1.5S.5M60	1400	1.5	2#12mm dia.	0.55
A1.5S1M60			2#10mm+2#12 mm dia.	1.0
A1.5S2M60			4#16 mm dia.	2.1
A1.5S3M60			6#16 mm dia.	3.1
A1.5S4M60			8#16 mm dia.	4.1
A2.5S.5M60	1930	2.5	2#12mm dia.	0.55
A2.5S1M60			2#10 mm+2#12 mm dia.	1.0
A2.5S2M60			4#16 mm dia.	2.1
A2.5S3M60			6#16 mm dia.	3.1
A2.5S4M60			8#16 mm dia.	4.1
A3.5S.5M60	2460	3.5	2#12 mm dia.	0.55
A3.5S1M60			2#10 mm+2#12 mm dia.	1.0
A3.5S2M60			4#16mm dia.	2.1
A3.5S3M60			6#16mm dia.	3.1
A3.5S4M60			8#16mm dia.	4.1
For all beams, width=150mm, overall depth=300mm, effective depth=265mm				

Cross sections of all the beams were kept constant at 150 x 300mm, while longitudinal reinforcement percentage ( $\rho_w=100A_s/bd$ ) was varied between 0.55 to 4.1. To avoid flexural failure, beams were adequately reinforced in the central 60 mm length. Fig. 1 shows typical longitudinal and sectional reinforcement configuration. Ribbed steel bars of Fe500 grade<sup>[6]</sup> with a diameter of 8, 10, 12, and 16mm were used. The ribbed bars had average yield strength of 588 MPa and an average tensile strength of 712 MPa. Sufficient anchorage length was provided by using 'L' and 'U' shaped hooks at the ends of the longitudinal reinforcement bars in all the beams, to minimize the possibility of a premature failure due to loss of end anchorage.

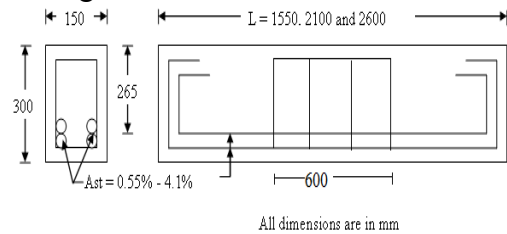


Fig. 1. Typical section and reinforcement layout of beam specimens

### 1.2 Materials and Mix Proportion

All the SCC beams were cast with 43-grade Ordinary Portland Cement (OPC) with specific gravity 3.12 and Blaine's fineness 4300cm<sup>2</sup>/gm<sup>[7]</sup>. To increase the powder content, anthracite fly ash which is a Class F fly ash having fineness 5000 cm<sup>2</sup>/gm<sup>[8]</sup> was added. For strength improvement micro-silica of Grade 920 U and having fineness 19200cm<sup>2</sup>/gm<sup>[9]</sup> was used. The coarse aggregate consisted of combination of 16 mm and 12mm crushed sandstone having specific gravity 2.59 and water absorption 0.80%<sup>[10, 11]</sup>. Fine aggregate used was natural river sand having specific gravity 2.63 and water absorption 1.18%<sup>[10, 11]</sup>. For self compaction and high fluidity,

modified poly carboxylic ether with a specific gravity of 1.055<sup>[12]</sup> was used as high range water reducing admixture. The mixture was prepared in the lab using a pan mixer of 200 liter capacity. It was empirically designed for 28-day nominal cylinder strength of 60 MPa and is presented in Table 2. The fresh properties of the SCC mixture was evaluated in terms of flow ability, pass ability and stability and the test results compiled in Table 3 indicate that the mixture was able to achieve suitable self-compact ability. Using steel forms, specimens were cast without any compaction, with concrete being poured in the formwork from one side until it flowed and reached the other side.

Table 2. Mix proportions

Cement, OPC 43 grade (kg/m <sup>3</sup> )	Fly ash (kg/m <sup>3</sup> )	Silica fume (kg/m <sup>3</sup> )	Total powder (kg/m <sup>3</sup> )	Fine agg. (kg/m <sup>3</sup> )	Coarse agg. (kg/m <sup>3</sup> )		Total agg. (kg/m <sup>3</sup> )	Water (kg/m <sup>3</sup> )
					16mm	12mm		
410	190	40	640	795	330	490	1615	165

Table 3. Fresh and hardened properties of SCC mixtures

Slump flow dia. (mm)	T500mm slump flow (s)	V-funnel Time (s)	U-Box height difference (mm)	J-ring height difference (mm)	GTM screen stability (%)	V-funnel at T <sub>5min</sub> (s)	Comp. strength, 28 day (MPa)	Split tensile strength, 28 day (MPa)
685	4.42	5.61	0	0	10.35	11.14	61.4	4.12

T500- time to achieve 500 mm slump flow, V funnel- time to empty funnel, V funnel at T<sub>5min</sub>-time to empty funnel after 5min. of filling

### 1.3 Test Set-Up and Instrumentation

The beams were tested as simply supported members under a four-point loading configuration. Fig.2 shows the photograph of a typical test setup in the lab. A stiff spreader beam was used to transfer the loads from the hydraulic ram to the test beams. The monotonically increasing load was applied in load-controlled mode until failure. The load-points and mid-span deflections were recorded with the help of linear variable

differential transformers (LVDT). All beams were instrumented to measure applied loads, deflections and crack widths.



Fig.2. Test setup, instrumentation and testing of beam specimen

The downward deflection of beams was monitored with the help of 3 LVDT's placed in the central portion of the beam, while formation and development of diagonal cracks was monitored with the help of LVDT's attached diagonally (two each) on the side face of shear spans of the beams(Fig. 2).

**2. RESULTS AND DISCUSSION:**

**2.1 Crack Pattern and Failure Modes**

Ultimate shear failure load of experimental beams is shown in column 4 of table 4. Being adequately reinforced in the central part, all beams failed in shear, with failure occurring when the inclined flexure-shear crack penetrated the compression zone of the beam near the loading plate. As the load was increased, the crack progression in the beams began with the appearance of fine flexural cracks in the central maximum moment region, followed by additional flexural cracks forming between the load and support regions. In all the experimental beams, shear failure occurred shortly after the formation of a dominant diagonal crack within the shear span.

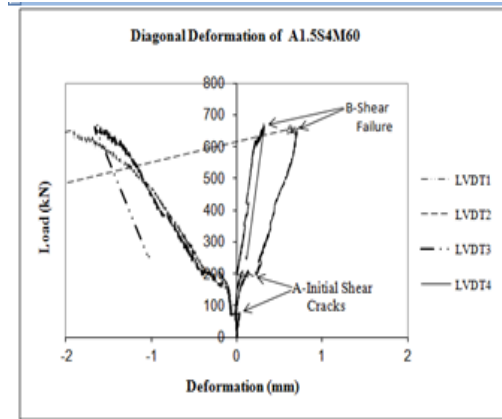


Fig. 3. Load deformation behavior of diagonal LVDT

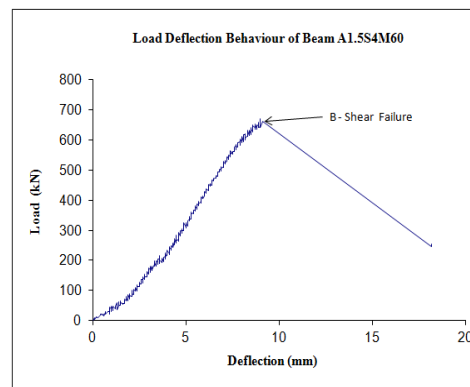


Fig. 4. Load deflection behavior of beam

Formation of shear cracks resulted in a sudden change in displacement in the LVDT's attached diagonally on the side face of the beam specimen (marked A in Fig. 3). Table 4 summarizes compressive strength ( $f_c'$ ), average ultimate shear stress at failure ( $v_u$ ), ratio of the average shear stress to compressive strength ( $v_u/f_c'$ ) and ratio of the average shear stress to square root of the compressive strength ( $v_u/\sqrt{f_c'}$ ).

Table 4. Shear strength of SCC beams from experiment

Beam designation	Compressive strength, $f_c'$ (MPa)	1st crack shear load, $V_{cr}$ (kN)	Ultimate shear load, $V_u$ (kN)	Ultimate shear stress, $v_u$ (MPa)	Norm. ultimate shear stress ( $v_{un}$ ) $v_u/f_c'$ (MPa)	Norm. ultimate shear Stress ( $v_{un}$ ) $v_u/\sqrt{f_c'}$ (MPa)
A1.5S.5M60	62.7	60.5	124.21	3.07	0.05	0.40
A1.5S1M60	61.5	69.8	168.68	4.17	0.07	0.53
A1.5S2M60	61.8	100.0	254.58	6.29	0.10	0.80
A1.5S3M60	60.2	89.0	327.12	8.08	0.13	1.04

A1.5S4M60	59.2	98.7	343.36	8.48	0.14	1.10
A2.5S.5M60	58.8	31.6	51.15	1.26	0.02	0.17
A2.5S1M60	62.2	47.6	66.99	1.65	0.03	0.21
A2.5S2M60	60.5	74.5	105.50	2.61	0.04	0.33
A2.5S3M60	58.8	81.5	142.72	3.52	0.06	0.46
A2.5S4M60	62.9	96.7	153.58	3.79	0.06	0.48
A3.5S.5M60	60.8	36.86	36.86	0.91	0.01	0.12
A3.5S1M60	58.8	47.99	47.99	1.19	0.02	0.15
A3.5S2M60	60.5	74.68	74.68	1.84	0.03	0.24
A3.5S3M60	60.8	88.49	88.49	2.19	0.04	0.28
A3.5S4M60	59.9	92.26	92.26	2.28	0.04	0.30

### 2.2 Shear Resistance Characteristics of SCC Beams

Since the section and concrete grade of all the beams under investigation was kept constant, the shear resistance of the beams was found to be strongly influenced by shear span to depth ratio(a/d) and longitudinal reinforcement percentage( $\rho_w$ ). Fig. 5 shows that for all the three a/d values, there is an increase in  $v_{un}$  with the increase in  $\rho_w$ , but with a difference in steepness of curves for different a/d values. This increase in  $v_{un}$  is due to enhanced dowel action and better aggregate interlocking in beam specimens having higher longitudinal reinforcement. For a short beam the influence of increase in longitudinal reinforcement on shear strength is more as compared to longer beams. For a/d = 1.5, there is a 175% increase in  $v_{un}$  with increase in  $\rho_w$  from 0.55 to 4.1, while this increase is 150% for a/d=3.5. This is due to a difference in shear transfer mechanism in SCC beams for different a/d ratios. At a/d= 1.5, shear strength is due to arch action mechanism, while in beams with a/d  $\geq$  2.5, the shear strength is due to cantilever mechanism. From Fig. 5 it is also seen that for all a/d values steepness of  $\rho_w$ - $v_{un}$  curves changes at  $\rho_w = 3.1$ , indicating its diminishing effect on shear strength at higher longitudinal reinforcement.

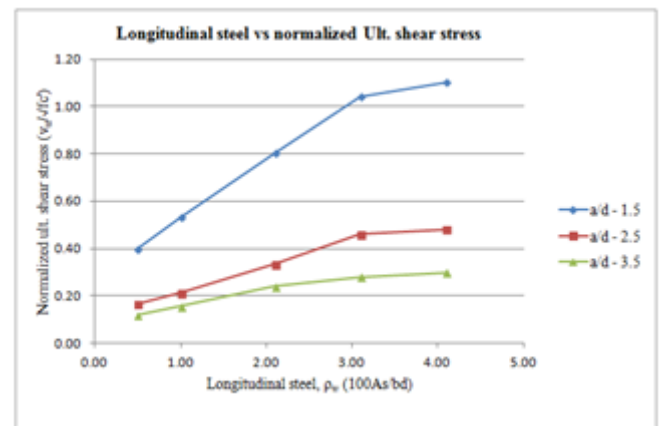


Fig.5. Longitudinal steel vs norm. ult. shear stress

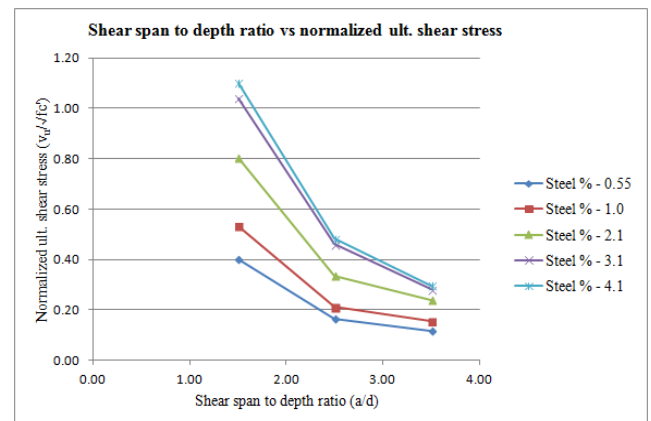


Fig. 6. Shear span to depth ratio vs norm. ult. shear stress

### 2.3 Effect of Longitudinal Reinforcement on Shear Strength

Column 4 of table 5 presents the ratio of ultimate to 1<sup>st</sup> crack shear stress ( $v_u^{exp}/v_{crack}$ ) values of different beam specimen. It can be seen that for the short

and medium span beams ( $a/d = 1.5$  and  $2.5$ ) having higher longitudinal reinforcement, the post-cracking shear resistance through dowel action and un-cracked concrete in compression zone is higher compared to beams having lower longitudinal reinforcement. But this trend of increase in  $v_u^{exp}/v_{crack}$  with increase in  $\rho_w$  is more pronounced upto  $\rho_w$  value of 3.1, indicating that contribution of dowel action on shear strength is more effective upto  $\rho_w = 3.1$ . For longer beams ( $a/d = 3.5$ ) the value of  $v_u^{exp}/v_{crack}$  is 1 for all values of  $\rho_w$ , which shows that in a cracked beam the dowel action has no effect on shear strength irrespective of longitudinal reinforcement percentage. As seen from Table 4, there is an increase in the shear resistance of the beam sections with the increase in longitudinal reinforcement percentage from 0.55 to 4.1. This behavior

is due to combination of enhanced dowel action, tighter shear cracks resulting into enhanced aggregate interlocking and a bigger concrete compression zone due to downward shifting of neutral axis. The increase is much steeper in experimental observations as compared to predicted values based on various expressions. From table 5, the experimental results indicate 150-200% increase in shear strength with  $\rho_w$  changing from 0.55 to 4.1, while the same is not reflected in ACI<sup>[12]</sup> and CSA<sup>[13, 14]</sup> expressions where an average increase of 35% has been computed. Expressions proposed by other researchers i.e. Bazant<sup>[15]</sup>, Zsutty<sup>[16, 17]</sup>, Zarasis<sup>[5]</sup>, Kim<sup>[18]</sup> and code base expressions i.e. JSCE<sup>[19]</sup> and CEB-FIP<sup>[20]</sup> shows 100-135% increase in shear strength, which reflects the trend of experimental results.

Table 5. Experimental and predicted shear capacities of beams with different shear span to depth ratio and longitudinal reinforcement

Beam designation	$v_u^{exp}$ (MPa)	$v_{crack}$ (MPa)	$\frac{v_u^{exp}}{v_{crack}}$	$\frac{v_u^{exp}}{v_{CSA}}$	$\frac{v_u^{exp}}{v_{ACI}}$	$\frac{v_u^{exp}}{v_{JSCE}}$	$\frac{v_u^{exp}}{v_{CEB-FIP}}$	$\frac{v_u^{exp}}{v_{AASHTO}}$	$\frac{v_u^{exp}}{v_{ZARASIS}}$	$\frac{v_u^{exp}}{v_{BAZANT}}$	$\frac{v_u^{exp}}{v_{ZSUTTY}}$	$\frac{v_u^{exp}}{v_{KIM}}$
A1.5S.5M60	3.0	1.76	1.7	3.2	2.6	3.58	2.83	2.95	2.98	1.89	1.43	1.35
A1.5S1M60	4.1	2.02	2.0	3.9	3.	3.88	3.06	2.87	3.03	1.72	1.55	1.42
A1.5S2M60	6.2	2.49	2.5	5.2	4.7	4.55	3.59	3.02	3.37	1.63	1.83	1.61
A1.5S3M60	8.0	2.85	2.8	6.3	5.5	5.11	4.04	3.59	3.74	1.62	2.06	1.78
A1.5S4M60	8.4	2.92	2.9	6.3	5.4	4.89	3.86	3.7	3.55	1.4	1.97	1.69
A2.5S.5M60	1.2	1.14	1.1	1.3	1.1	1.5	1.4	1.66	1.29	1.18	1.18	1.17
A2.5S1M60	1.6	1.41	1.1	1.5	1.4	1.54	1.44	1.28	1.26	1.12	1.22	1.16
A2.5S2M60	2.6	2.02	1.2	2.2	2.1	1.89	1.77	1.37	1.48	1.25	1.5	1.38
A2.5S3M60	3.52	2.28	1.54	2.79	2.71	2.24	2.09	1.72	1.72	1.38	1.78	1.61
A2.5S4M60	3.79	2.41	1.57	2.81	2.75	2.18	2.04	1.67	1.65	1.28	1.74	1.54
A3.5S.5M60	0.91	0.91	1.00	0.97	0.81	1.06	1.11	1.54	0.98	0.94	0.94	1.23
A3.5S1M60	1.19	1.19	1.00	1.11	1.04	1.1	1.15	1.06	0.95	0.93	0.97	1.23
A3.5S2M60	1.84	1.84	1.00	1.54	1.53	1.33	1.39	1.05	1.08	1.07	1.18	1.44
A3.5S3M60	2.19	2.19	1.00	1.7	1.73	1.36	1.43	1.07	1.08	1.06	1.21	1.46
A3.5S4M60	2.28	2.28	1.00	1.69	1.76	1.31	1.37	1.02	1.04	0.99	1.17	1.38

Bazant's<sup>[15]</sup> fracture mechanics based formula which is also called size effect law, predicts ultimate shear strength with good precision, having  $v_u^{exp}/v_u^{pred}$  values lying between 0.94 and 1.89. The expression includes the effect of aggregate

size and beam depth along with reinforcement ratio and beam size. Zsutty's<sup>[16]</sup> method, which is based on multiple regression analysis, also follows the experimental shear strength values quite closely. The reason being that Zsutty

has proposed two separate equations for predicting ultimate shear, one for beams with  $a/d \leq 2.5$  and the other for the beams with  $a/d > 2.5$ . Columns 5-9 of Table 5 presents ratio of experimental to code based provisions ( $v_u^{exp}/v_u^{pred}$ ) of different standards, from which different trends can be observed for different  $a/d$  values. For  $a/d = 1.5$ , the codal provisions of various standards are highly conservative in estimation of ultimate shear stress with ( $v_u^{exp}/v_u^{pred}$ ) lying between 3.0 to 6.4. For  $a/d = 2.5$ , codal expressions are less conservative in estimating shear strength, particularly for lightly reinforced sections.

**2.4 Effect of Shear Span to Depth Ratio on Shear Strength**

Different graphs have been plotted for different  $\rho_w$  values. Fig 7-8 shows a much larger decrease in experimental ultimate shear stress ( $v_u^{exp}$ ) as compared to predicted shear stress ( $v_u^{pred}$ ) values calculated by using different expressions. An average decrease of 58% and 32% is observed in  $v_u^{exp}$  when  $a/d$  increases from 1.5 to 2.5 and 2.5 to 3.5 respectively. Except Kim, Bazant and Zsutty other equations show little or no dependence of shear stress on  $a/d$  value. Using Kim equation, 67% decrease in shear strength is seen when  $a/d$  increases from 1.5 to 3.5, which closely follows the experimental results where a decrease of 71% is seen. With Zsutty equation a decrease of 54% is seen, while change in  $a/d$  has little or no effect on shear stress using ACI, CSA or JSCE equations.

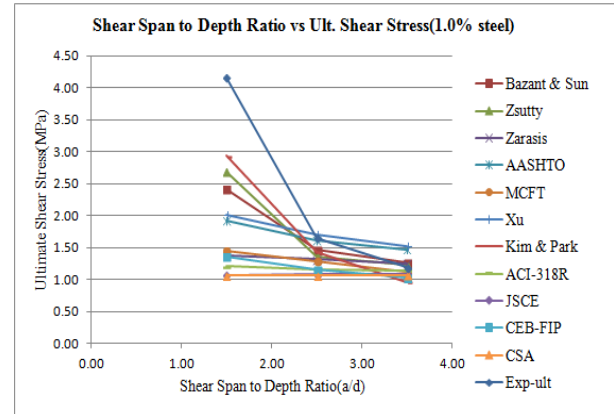


Fig. 7.  $a/d$  ratio v/s ult. shear stress (1.0% steel)

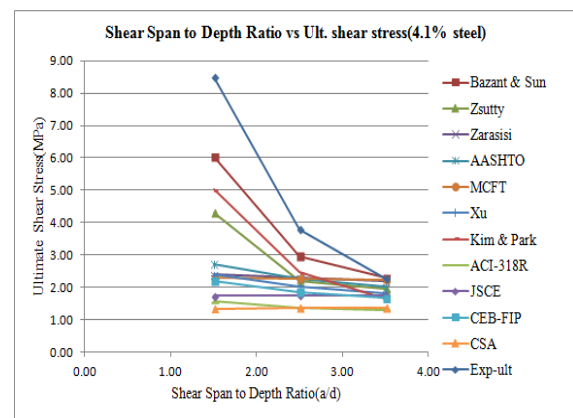


Fig. 8.  $a/d$  ratio v/s ult. Shear stress (4.1% steel)

According to Table 6, regardless of the percentage of longitudinal reinforcement the expression used to calculate  $v_u^{pred}$ , there is a decrease in the value of  $v_u^{exp}/v_u^{pred}$  with increase in  $a/d$  value. In other words it can be said that with a decrease in value of  $a/d$ , the calculated shear strength values become more and more conservative. This is mainly attributable to the higher contribution of the arch action mechanism at lower  $a/d$  ratios, which is ignored by most shear design methods.

**CONCLUSIONS:**

Based on crack pattern, crack load, failure modes and overall shear resistance of beam specimen under investigation, the following conclusions can be drawn:

- Variation of shear strength with change in longitudinal reinforcement

is more pronounced in short span beams as compared to longer beams. At higher percentage of longitudinal reinforcement ( $\rho_w > 3.1$ ), the contribution of longitudinal reinforcement to shear strength diminishes.

- Irrespective of the value of  $a/d$  or longitudinal steel percentage, the equation proposed by Kim was found to give most accurate in prediction of the shear strength of all beams under the current experimental investigation.
- Existing code based expressions of JSCE, AASHTO and CEB-FIP for calculating contribution to shear strength of normally vibrated concrete beams can be safely applied to high strength SCC beams. Except for lightly reinforced long span beams, ACI and CSA expressions can also be safely used for predicting shear strength of high strength SCC beams. All code based expressions are very conservative in predicting shear strength of short span SCC beams in high strength range, whereas for longer beams the predicted values are close to experimental results.

## REFERENCES:

- (1) Mphonde, A.G.; Frantz, G.C. 1984. *Shear Strength of High Strength Reinforced Concrete Beams (Report CE 84-157)*, Civil Engineering Department, University of Connecticut, Storrs, CT, Jun. 1984, 260 pp.
- (2) Hassan, A.A.A.; Hossain, K.M.A.; Lachemi, M. 2008. *Behavior of full-scale self-consolidating concrete beams in shear*, *Cement & Concrete Composites* 30: 588–596.
- (3) Lachemi, M.; Hossain, K.M.A.; Lambros, V. 2005. *Shear resistance of self-consolidating concrete beams- Experimental investigations*. *Canadian Journal of Civil Engineering* 32(6): 1103-1113.
- (4) Choulli, Y.; Mari', A. R.; & Cladera, A. 2008. *Shear behavior of full-scale pre-stressed I-beams made with self-compacting concrete*. *Materials and Structures*, 41, 131–141.
- (5) Zararis, P.D.; Papadakis, GC. 2001. *Diagonal shear failure and size effect in RC beams without web reinforcement*. *ASCE, Journal of Structural Division*. 127(7): 733–741.
- (6) IS: 1786(2008): *Specifications for high strength deformed steel bars and wires for concrete reinforcement*, New Delhi, India.
- (7) IS: 8112(1989), *Ordinary Portland Cement, 43 Grade — Specification*, New Delhi, India.
- (8) IS: 3812(2013), *Specification for pulverized fuel ash: Part 1 for use as pozzolana in cement, cement mortar and concrete (third revision)*, New Delhi, India.
- (9) IS: 15388(2003), *Silica Fume-Specification*, New Delhi, India.
- (10) IS: 383(1970, R2011), *Specification for coarse and fine aggregates from natural sources for concrete*, New Delhi, India.
- (11) IS: 9103(1999), *Concrete admixtures-Specification, (Reaffirmed 2004)*, New Delhi, India.
- (12) ACI 211.1-91(1998, Reaffirmed 2002), *Standard practice for selecting proportions for normal, heavyweight and mass concrete*. American Concrete Institute, Farmington Hills, Michigan, America.
- (13) American Concrete Institute ACI Committee(2011): *Building code requirements for structural concrete ACI 318-11 and commentary 318R-11*. Farmington Hills, MI: American Concrete Institute.
- (14) Canadian Standard Association, CSA(2004). *Design of concrete structures*. CSA standard A23.3-04. Rexdale (ON).
- (15) Bazant, Z. P.; Sun, H.H. 1987. *Size effect in diagonal shear failure: Influence of aggregate size and stirrups*. *ACI Journal*. 84(4), 259–272.
- (16) Zsutty, T.C. 1968. *Beam shear strength prediction by analysis of existing data*. *ACI Structural Journal* 65: 943–51.
- (17) Zsutty, TC. 1971. *Shear strength prediction for separate categories of simple beam tests*. *ACI Structural Journal* 68: 138–143.
- (18) Kim, J.K.; Park, Y.D. 1996. *Prediction of shear strength of reinforced concrete beams without web reinforcement*. *ACI Materials Journal* 93(3): 213-222.
- (19) Japan Society of Civil Engineers. *Standard specification for concrete structure*. Japanese Society of Civil Engineering No. 15, Tokyo. 2007: p. 154–59.
- (20) CEB-FIP model code 1990. *Comité Euro-International du Béton/Federation internationale de la precontrainte*. UK: Thomas Telford London; 1993. p. 437.